JCI The Journal of Clinical Investigation

Published in Volume 122, Issue 1 (January 3, 2012)
J Clin Invest. 2012;122(1):218–228. doi:10.1172/JCI59072.

Research Article

Histamine-releasing factor has a proinflammatory role in mouse models of asthma and allergy

Jun-ichi Kashiwakura[1,2], Tomoaki Ando[1], Kenji Matsumoto[3], Miho Kimura[1], Jiro Kitaura[1], Michael H. Matho[1], Dirk M. Zajonc[1], Tomomitsu Ozeki[4], Chisei Ra[2], Susan M. MacDonald[5], Reuben P. Siraganian[6], David H. Broide[7], Yuko Kawakami[1] and Toshiaki Kawakami[1]

[1]Division of Cell Biology, La Jolla Institute for Allergy and Immunology, La Jolla, California, USA.
[2]Division of Molecular Cell Immunology and Allergology, Advanced Medical Research Center, Nihon University Graduate School of Medical Science, Tokyo, Japan.
[3]Department of Allergy and Immunology, National Research Institute for Child Health and Development, Tokyo, Japan.
[4]ULVAC Inc., Chigasaki, Japan.
[5]Johns Hopkins Asthma and Allergy Center, Baltimore, Maryland, USA.
[6]Receptors and Signal Transduction Section, OIIB, National Institute for Dental and Craniofacial Research, NIH, Bethesda, Maryland, USA.
[7]Department of Medicine, UCSD, La Jolla, California, USA.

Address correspondence to: Toshiaki Kawakami, Division of Cell Biology, La Jolla Institute for Allergy and Immunology, 9420 Athena Circle, La Jolla, California 92037, USA. Phone: 858.752.6814; Fax: 858.752.6986; E-mail: toshi@liai.org.

Authorship note: Jun-ichi Kashiwakura and Tomoaki Ando contributed equally to this work.

First published December 1, 2011
Received for publication May 18, 2011, and accepted in revised form October 12, 2011.

IgE-mediated activation of mast cells and basophils underlies allergic diseases such as asthma. Histamine-releasing factor (HRF; also known as translationally controlled tumor protein [TCTP] and fortilin) has been implicated in late-phase allergic reactions (LPRs) and chronic allergic inflammation, but its functions during asthma are not well understood. Here, we identified a subset of IgE and IgG antibodies as HRF-interacting molecules in vitro. HRF was able to dimerize and bind to Igs via interactions of its N-terminal and internal regions with the Fab region of Igs. Therefore, HRF together with HRF-reactive IgE was able to activate mast cells in vitro. In mouse models of asthma and allergy, Ig-interacting HRF peptides that were shown to block HRF/Ig interactions in vitro inhibited IgE/HRF-induced mast cell activation and in vivo cutaneous anaphylaxis and airway inflammation. Intranasally

administered HRF recruited inflammatory immune cells to the lung in naive mice in a mast cell– and Fc receptor–dependent manner. These results indicate that HRF has a proinflammatory role in asthma and skin immediate hypersensitivity, leading us to suggest HRF as a potential therapeutic target.

Introduction

Mast cells and basophils are key effector cells for IgE-dependent allergic inflammatory reactions (1). Upon activation, these cells secrete preformed proinflammatory chemical mediators (e.g., histamine, proteases, proteoglycans, and nucleotides) as well as de novo synthesized lipids (e.g., leukotrienes and prostaglandins) and polypeptides (e.g., cytokines and chemokines). These substances lead to the development of allergic inflammation.

Since Thueson et al. first described an activity from cultured peripheral blood mononuclear cells that induced the release of histamine from basophils (2), histamine-releasing activities have been studied for more than 30 years (3). In addition to several cytokines and chemokines with this activity, an unrelated protein termed histamine-releasing factor (HRF) was purified and molecularly cloned in 1995 (4). HRF, also known as translationally controlled tumor protein (TCTP) and fortilin, is a highly conserved protein with both intracellular and extracellular functions (4–8). HRF is secreted by macrophages and other cell types and can stimulate histamine release and IL-4 and IL-13 production from IgE-sensitized basophils and mast cells (9). HRF-like activities were found in nasal, skin blister, and bronchoalveolar lavage (BAL) fluids during late-phase allergic reactions (LPRs), implicating HRF in the LPR and chronic allergic inflammation (10–12). However, definitive evidence for the role of HRF in allergic reactions has been elusive (8, 9, 13).

Confounding the research, HRF has a wide range of intracellular functions, including cell cycle progression, proliferation, survival, and malignant transformation of a variety of cell types (8). HRF is ubiquitously expressed in all tested eukaryotic cells; its expression is active in mitotically active tissues (14, 15) and subject to both transcriptional and translational control (16). In tumor cells, HRF is highly expressed and downregulated upon tumor reversion (17). It is involved in the elongation step of protein synthesis by interacting with both eEF1A (a small GTPase) and eEF1Bβ (a guanine nucleotide exchange factor) (18–20). Drosophila and human HRFs act as the guanine nucleotide exchange factor for the Ras superfamily GTPase, Rheb, which regulates the TSC1-TSC2-mTOR pathway (21, 22). These studies implicate this protein in the regulation of growth and proliferation as well as in the control of organ size. HRF interacts with Mcl-1 (23, 24) and Bcl-xL (25), antiapoptotic members of the Bcl-2 family, and antagonizes apoptosis by inserting into the mitochondrial membrane and inhibiting Bax dimerization (26). HRF also interacts with p53 tumor suppressor and suppresses p53-mediated apoptosis (27). Other HRF-interacting molecules include tubulin (28), NEMO (29) and vitamin D_3 receptor (30). Phosphorylation of HRF by the protein kinase Plk decreases the microtubule-stabilizing activity of HRF (31).

The extracellular function of HRF is considered a cytokine-like activity toward IgE-primed mast cells and basophils (9). Despite considerable efforts, researchers have failed to identify an HRF receptor. Unfortunately, HRF knockout mice are embryonic lethal (32, 33) and cannot provide meaningful information on HRF function. Because of the lack of reagents that can distinguish between HRF's intracellular and extracellular functions, it is particularly difficult to dissect extracellular functions in complex in vivo settings. In this study, we sought to identify HRF-interacting molecules and inhibitors of interactions of HRF with HRF-reactive molecules.

Results

HRF binds to Fab fragments of a subset of IgE and IgG antibodies. Despite a previous study implying that IgE does not interact with HRF (34), we reexamined this possibility first by using an ELISA and a panel of IgE mAbs. As shown in Figure 1A, immobilized N-terminally glutathione S-transferase–tagged (GST-tagged) mouse HRF protein (referred to herein as GST-mHRF) bound C38-2 and 5 other IgE mAbs. In contrast, C48-2 and 12 other IgE mAbs failed to bind GST-mHRF. Similar results were obtained when C-terminally

hexahistidine-tagged mHRF (referred to herein as mHRF-His_6) was used as a capturing agent (Supplemental Figure 1; supplemental material available online with this article; doi: 10.1172/JCI59072DS1). Interaction of C38-2 and IGELa2 IgE mAbs with mHRF was also demonstrated by affinity pulldown (Figure 1B and data not shown). HRF bound to mouse bone marrow–derived mast cells (BMMCs) preincubated with the HRF-reactive C38-2 IgE, but not the HRF-nonreactive C48-2 IgE, in flow cytometry experiments (Figure 1C). However, we observed no HRF binding to C38-2 IgE–incubated *FcεRIα–/–* BMMCs, which lack expression of the high-affinity IgE receptor FcεRI. We also found that 9 of the 34 tested IgG mAbs bound to mHRF (Figure 1D). HRF binding was independent of IgG isotype or antigen specificity. For example, the HRF-binding IgG molecules JK31 and JK96, and the non-HRF binding IgG molecule JK116 all recognize the same viral antigen.

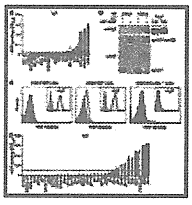

Figure 1

A subset of IgE and IgG molecules binds HRF.(**A**) IgE molecules were incubated in GST-mHRF–coated wells. HRF-bound IgE was quantified by ELISA, as detected by color development with HRP. OD_{450} values with GST-mHRF subtracted from those with GST control are shown. $OD_{450} \leq 0.1$ was used as an arbitrary cutoff value. Data represent at least 3 experiments. (**B**) IgEs were incubated with GST- or GST-mHRF–agarose beads. Bead-bound IgEs were pulled down. IgE and GST proteins were detected by immunoblotting. Lanes were run on the same gel but were noncontiguous (white lines). Representative of 2 experiments. (**C**) BMMCs preincubated with (black line) or without (gray shading) the indicated IgE (see Supplemental Table 3) were incubated with mHRF-His_6, and bound mHRF-His_6 was detected with rabbit anti-His tag antibody and Alexa Fluor 647–conjugated anti-rabbit IgG. HRF binding was detected by flow cytometry. Insets show IgE binding: the same cells were incubated with FITC-labeled anti-mouse IgE. Representative of 2 experiments. (**D**) HRF-bound IgGs were detected by ELISA. Representative of 3 experiments. HRF binding was independent of IgG isotype, as the tested IgG1, IgG2a, and IgG2b molecules contained both HRF-reactive and -nonreactive molecules. The K_D values for HRF binding were 0.685 μM (JK17), 2.78 μM (JK31), and 5.78 μM (JK96). Black bars, IgG1; white bars, IgG2a; gray bars, IgG2b.

- View PDF

Importantly, an Fab, but not Fc, fragment of an HRF-binding IgG molecule bound mHRF (Figure 2, A and B), and the IgE-HRF (or IgG-HRF) interaction was inhibited by an Fab, but not Fc, fragment (Figure 2, C–F). Consistent with this, the interaction between the OVA-specific αOE IgE and mHRF was inhibited by OVA (Supplemental Figure 2A), and those between the trinitrophenyl-specific (TNP-specific) IGELa2 or C38-2 IgE and mHRF were inhibited by TNP-glycine (Supplemental Figure 2, C and E). However, the IGELa2-mHRF and C38-2–mHRF interactions were not inhibited by TNP–glutamic acid (Supplemental Figure 2, C and E), and the C38-2–mHRF interaction was not inhibited by TNP-lysine, whereas the IGELa2-mHRF interaction was inhibited by TNP-lysine. These results suggest that the mHRF-binding site in IgE overlaps at least in part with the antigen-binding sites. Collectively, these results suggest that a considerable proportion of antibodies in immunized mice interact with HRF. In addition, 1 of the 5 tested human IgEs (i.e., HE-1) bound GST-mHRF (data not shown).

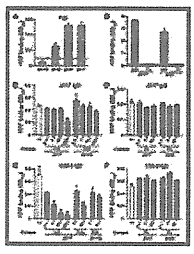

Figure 2

HRF-reactive Igs binds HRF via their Fab region.(**A** and **B**) Fab, but not Fc, fragments bound to HRF. GST-mHRF was coated onto a 96-well ELISA plate. After blocking with 10% FCS, the plate was incubated with whole molecules (IgG) or with Fab or Fc fragments of the indicated IgGs. HRF-bound Fab was detected by incubation with HRP-conjugated goat anti-mouse κ chain antibody. HRF-bound Fc or IgG was detected with HRP-conjugated anti-IgG. (**C** and **D**) Competition by Fab, but not Fc, fragments for JK17 IgG binding to HRF. GST-mHRF was incubated with JK17 IgG in the presence or absence of Fab or Fc fragments at different molar ratios. Bound JK17 IgG was detected with HRP-conjugated anti-κ (**C**) or biotin-conjugated anti-IgG1 followed by streptavidin-HRP (**D**). (**E** and **F**) Competition by Fab, but not Fc, fragments for C38-2 IgE binding to HRF. GST-mHRF was incubated with C38-2 IgE in the presence or absence of Fab or Fc fragments at

different molar ratios. Bound IgE was detected with biotin-conjugated anti-mouse IgE followed by streptavidin-HRP. $*P < 0.05$. All data are representative of 2 experiments.

Peptides corresponding to the Ig-binding sites within HRF inhibit HRF-Ig interactions. We next mapped the Ig-binding sites within HRF. IgE and IgG binding assays using a panel of truncated GST-mHRF proteins gave similar binding patterns (Figure 3, A and B, and Supplemental Figure 3). A major Ig-binding site was mapped to the N-terminal 19-residue peptide (N19), as GST-tagged N19 (referred to herein as GST-N19), but not GST fusion proteins containing shorter N-terminal fragments, bound Igs. Another binding site was mapped to internal residues 79–142 (Figure 3, A and B). Further fine mapping localized the latter binding site to the H3 region (residues 107–135, termed GST-H3; Figure 3D and data not shown).

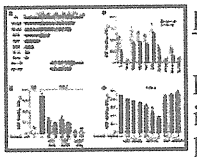

Figure 3

Mapping IgE-binding sites within HRF and inhibition of HRF-IgE interactions by the HRF-derived N19 and H3 peptides.(**A**) Scheme of full-length (FL) and truncated forms of GST-mHRF used for binding assays. Domain structures such as TCTP1–TCTP2 and H1–H3 are shown. (**B**) IgE-binding site mapping. C38-2 (5 μg/ml) and αOE (20 μg/ml) IgE molecules were incubated in wells coated with GST-mHRF. Bound Igs were detected by ELISA. <0.1, value too small to display. (**C**) Inhibition of HRF-Ig interactions by N19. IgE molecules were incubated in GST-mHRF–coated wells in the presence or absence of the indicated concentrations of competitors. After incubation, bound IgE was detected by ELISA. (**D**) Inhibition of HRF-Ig interactions by GST-H3. $*P < 0.05$, $**P < 0.01$. Data are representative of 2 (**B**), 5 (**C**), or 3 (**D**) experiments.

Intracellular HRF might contribute to allergic inflammation by controlling cell cycle progression, proliferation, and survival of immune and structural cells (8, 21, 32). Therefore, it is essential to find an inhibitor of HRF-Ig interactions to dissect HRF's extracellular functions, separate from HRF's intracellular functions. We tested whether the Ig-interacting HRF sequences might serve as specific inhibitors of HRF binding to Igs. Indeed, GST-N19 inhibited IgE binding to mHRF with potency similar to full-length GST-mHRF (Figure 3C). However, shorter mHRF peptides tested (residues 1–6, 1–12, 1–16, 5–19, and 9–19) or a scrambled peptide (KYI-N16) did not inhibit HRF-IgE binding (Supplemental Figure 4). Control experiments showed that GST-N19 did not affect growth properties that fall under the control of intracellular functions of HRF (8): treatment of various cells with 3.6 or 36 μM GST-N19 did not affect their viability or proliferation (Supplemental Figure 5, A–D), nor did it affect apoptosis induced by growth factor withdrawal in BMMCs or by H_2O_2 in CHO-K1 cells (Supplemental Figure 5, E and F). These concentrations of HRF were higher than what has previously been shown to stimulate basophils (1.6–5 μM; ref. 35). Importantly, GST-N19 did not enter BMMCs (Figure 4A). A synthetic N19 peptide also inhibited IgE binding to mHRF and did not alter the growth or survival of various cells (Supplemental Figure 6). Similar to GST-N19, GST-H3 also inhibited IgE binding to mHRF (Figure 3D); GST-H3 neither affected cell growth or apoptosis nor entered the cells (Supplemental Figure 7 and data not shown). These results indicated that the HRF N19 and H3 peptides can be used to probe extracellular functions of HRF in vitro and in vivo.

• Cite this article

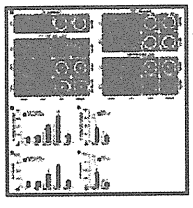

Figure 4

GST-N19 does not enter the cell interior and serves as an HRF inhibitor.(**A**) BMMCs were incubated with TAT-GST, GST, or GST-N19 protein for the indicated time periods at 37°C. Washed cells were fixed, permeabilized, and stained with anti-GST followed by Alexa Fluor 488–conjugated anti-mouse IgG. Nuclei were stained with DAPI. Fluorescence was observed by confocal microscopy. DIC, differential interference contrast. Original magnification, ×150. Percentages of the cells similar to the representative images are shown (≥150 cells scored). (**B** and **C**) BMMCs were incubated with 5 μg/ml of the indicated IgE and 100 μg/ml mHRF for 45 minutes (histamine release) or 20 hours (IL-6 production). (**D** and **E**) BMMCs were incubated with IgE and mHRF in the presence of 100 μM GST or GST-N19. $*P < 0.05$, $**P < 0.01$ versus respective control, Student's t test. Data are representative of 3 (**A**) or 2 (**B**–**E**) experiments.

N19 and H3 peptides block mast cell activation. Analysis of purified recombinant mHRF-His_6 on reducing and nonreducing SDS-PAGE yielded direct evidence for disulfide-linked dimerization of HRF (Supplemental Figure 8A). Both monomeric and dimeric forms of HRF could bind to IgE (data not shown). Consistent with this, monomeric mHRF mutant 2CA, with 2 cysteine residues at positions 28 and 172 substituted with alanine, also bound Igs (Supplemental Figure 9, A and B). The dimerizing ability of HRF with 2 Ig-binding sites suggests the potential of HRF to crosslink Ig-bound Fc receptors (Supplemental Figure 8B). This notion was supported by activation of mast cells by cotreatment with mHRF and HRF-reactive, but not HRF-nonreactive, IgEs, as evidenced by histamine release and cytokine production from BMMCs (Figure 4, B and C) and by β-hexosaminidase release from peritoneal mast cells (C38-2 IgE, 17.8% ± 4.6% release; C48-2 IgE, 2.4% ± 0.1% release; $P < 0.0001$). These reactions were inhibited by GST-N19 and GST-H3 (Figure 4, D and E, and data not shown). Consistent with mast cell activation, tyrosine phosphorylation of several proteins was observed in C38-2 IgE/HRF-treated cells (data not shown).

HRF inhibitors suppress passive cutaneous anaphylaxis. Acute passive cutaneous anaphylaxis (PCA) reactions induced by antigen in IgE-sensitized mice are mediated mainly by histamine released from activated mast cells (36). LPRs in the skin are mediated in part by mast cell–derived TNF-α (37, 38) and IL-33 (39). Strikingly, when HRF was injected i.d. 24 hours after IgE injection, both acute reactions and LPRs were induced by HRF-reactive, but not HRF-nonreactive, IgE (Figure 5, A and B). The HRF-reactive C38-2 IgE induced increased vascular permeability after HRF injection (Figure 5A). Interestingly, the LPRs induced by HRF, as measured by increased ear swelling at 6 hours, were as high as those induced by antigen (Figure 5B). Both acute reactions and LPRs induced by IgE/HRF were prevented by pretreatment with GST-N19 (Figure 5C and data not shown) and appeared to be mast cell mediated, as the reactions were abolished in mast cell–deficient $Kit^{W-sh/W-sh}$ mice (40) and restored in $Kit^{W-sh/W-sh}$ mice engrafted with WT BMMCs (Figure 5A). Furthermore, loss of FcεRI abolished PCA responses (Figure 5D). Control experiments showed little effect of GST or GST-N19 alone on ear thickness (data not shown). Therefore, HRF and HRF-reactive IgE can induce anaphylactic responses in a mast cell– and FcεRI-dependent manner. Interestingly, PCA reactions were not induced by IgE/2CA mutant (Supplemental Figure 9, C and D), and IgE/HRF-induced PCA reactions were inhibited by 2CA mutant (Supplemental Figure 9E), which suggests that the dimeric form of HRF is responsible for the bioactivity of HRF.

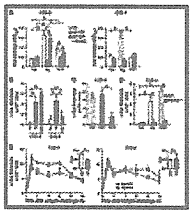

Figure 5

HRF promotes PCA reactions in mice sensitized with HRF-reactive IgE.(**A**) IgE/HRF-induced acute PCA reactions. Mice were sensitized with the indicated IgEs. 24 hours later, Evans blue and mHRF-His_6 were injected in IgE-sensitized mice. After 30 minutes, dye leakage from the ears was measured. For controls, saline (Sal) and TNP_{26}-BSA (Ag) were injected in sensitized ears. $Kit^{W-sh/W-sh}$ mice were used before or 6 weeks after engraftment of WT BMMCs by i.d. injection. Toluidine blue staining confirmed that the engrafted mice had numbers of mast cells similar to those of WT mice. (**B–D**) IgE/HRF-induced PCA LPRs. mHRF-His_6 was injected in IgE-sensitized ears, and LPR was analyzed by measurement of ear thickness at 6 hours. For controls, saline and TNP_{26}-BSA were injected. (**C**) C38-2 IgE–sensitized mice were pretreated with saline, GST, or GST-N19 (N19) before injection with mHRF-His_6. (**D**) LPR in $FcεRIα^{-/-}$ mice. (**E**) Inhibition of IgE/antigen-induced PCA reactions by GST-N19. WT mice were sensitized overnight with the indicated IgEs. Left ears were injected with GST and right ears were injected with GST-N19, then TNP_{26}-BSA was injected in both ears. Ear thickness was measured. Insets show area under curve (AUC). $^{*}P < 0.05$, $^{\#}P < 0.01$, $^{\S}P < 0.001$. 3–6 mice were used for each cohort. Data are representative of 2 (**A–D**) or 3 (**E**) experiments.

We next tested whether HRF contributes to IgE/antigen-induced PCA reactions. Antigen was injected to the ears of IgE-sensitized mice, with GST-N19 or GST pretreatment. GST-N19 significantly reduced PCA acute reactions and LPRs in mice sensitized with HRF-reactive IgE (Figure 5E and data not shown). However, PCA induced by an HRF-nonreactive IgE

was insensitive to GST-N19 treatment. Similar results were observed using GST-H3 in place of GST-N19, and GST-N19 plus GST-H3 had a stronger PCA-suppressive effect than GST-N19 or GST-H3 alone (Supplemental Figure 10). These results suggest that HRF is required for maximal IgE/antigen-induced PCA reactions. Consistent with this, HRF was dramatically increased in the dermis during LPRs (Supplemental Figure 11).

HRF inhibitors suppress mast cell–dependent airway inflammation. Asthma is a chronic lung disease characterized by airway inflammation, airway hyperresponsiveness (AHR), and reversible airway obstruction (41). We used a mast cell–dependent, OVA-induced airway inflammation model (42). In addition to the increased HRF levels in lungs and blood (Figure 6A), immunofluorescence microscopy showed increased levels of HRF staining in nonpermeabilized lung tissues (Supplemental Figure 12A), which indicates that HRF is secreted into lung tissues in OVA-challenged mice. Levels of HRF-reactive IgG were also increased in plasma and BAL fluids of these mice (Supplemental Figure 12B). Pretreatment with GST-N19 before the OVA challenges abrogated airway inflammation, as evidenced by reduced eosinophils and neutrophils in BAL fluids (Figure 6B) and by reduced inflammatory cells and goblet cell hyperplasia in the lung (Figure 6C). Production of IL-13 (the cytokine essential for AHR, eosinophilia, and mucus production; refs. 43–45) and IL-5 (the cytokine critical for eosinophilia and AHR; ref. 46) in lung tissues was drastically decreased in GST-N19–treated mice (Figure 6D). Consistent with these observations, GST-N19 treatment inhibited AHR ($P < 0.05$ vs. GST at 48 mg/ml methacholine, Bonferroni correction; Figure 6E). Circulating systemic HRF was reduced by GST-N19 (Supplemental Figure 12C), probably reflecting an antiinflammatory effect of GST-N19. In contrast, HRF-reactive plasma IgG levels and OVA-specific IgE, IgG1, and IgG2a levels were not affected by GST-N19 (Supplemental Figure 12B and data not shown). Administration of a synthetic N19 peptide or GST-H3 abrogated airway inflammation with similar potency to that of GST-N19 (Supplemental Figure 13 and data not shown).

article

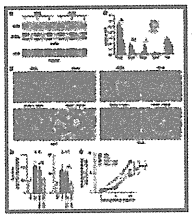

Figure 6

GST-N19 blocks mast cell–dependent airway inflammation.C57BL/6 mice were sensitized with OVA (10 μg) and i.n. challenged with OVA (20 μg) or PBS. Some mice were i.n. pretreated with GST or GST-N19 (400 μg) before every OVA challenge. 24 hours after the last challenge, mice were subjected to invasive lung function testing, and BAL fluids and lung tissues were collected. (**A**) Increased HRF amounts in the lung and sera of OVA-sensitized and -challenged mice. SDS-PAGE was performed on lung homogenates and serum samples, and HRF amounts of 3 mice were evaluated by immunoblotting. ERK1/2 expression was used as a loading control. (**B**) Total and specific immune cell numbers in BAL fluids. Eos, eosinophils; Neu, neutrophils; Lym, lymphocytes; MΦ, macrophages and monocytes. (**C**) H&E and periodic acid-Schiff (PAS) staining of lung tissues. Scale bars: 200 μm. (**D**) IL-5 and IL-13 in lung homogenates were measured by ELISA. (**E**) Airway resistance was measured using FlexiVent. $*P < 0.05$, $**P < 0.01$, $***P < 0.001$. 3–6 mice were used for each cohort. All data are representative of 3 experiments.

We confirmed the efficacy of GST-N19 in a second model of asthma: partially IgE-dependent airway inflammation induced by *Aspergillus fumigatus* allergens (47). HRF inhibition resulted in substantial reduction of allergic airway inflammation and inflammatory cells in BAL fluids (Supplemental Figure 14). Interestingly, HRF inhibition failed to reduce airway inflammation in a mast cell–independent OVA-alum model (ref. 48 and Supplemental Figure 15).

HRF-induced airway inflammation is dependent on Fc receptors. Airway inflammation in the above experiments involves a complex interplay of various cells (41, 49, 50). To gain mechanistic insights into how HRF promotes lung inflammation, we used a simpler in vivo model. Administration i.n. of WT, but not 2CA mutant, reduced/carboxymethylated or boiled mHRF to WT naive mice induced weak but consistent lung inflammation, as shown by increased eosinophils, neutrophils, and macrophages/monocytes in BAL fluids (Figure 7A and data not shown). However, no or little HRF-induced lung inflammation was seen in B cell–deficient (μ*MT*), mast cell–deficient ($Kit^{W\text{-}sh/W\text{-}sh}$), or $FcR\gamma^{-/-}$ mice (Figure 7, A and B). FcRγ is shared by multiple Fc receptors, including FcεRI, FcγRI, FcγRIII, and FcγRIV (51, 52). Among the Igs and Fc receptors, IgE and FcεRI were the predominant contributors

to the effects of HRF, as HRF-induced lung inflammation was almost abrogated in naive *FcεRIα*$^{-/-}$ mice (Figure 7A). Since FcεRI is expressed on mast cells and basophils in mice (53), these results were consistent with the effectiveness of N19 and H3 peptides in mast cell–dependent asthma models (Figure 6 and data not shown).

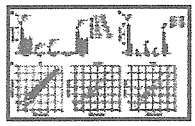

Figure 7

Lung inflammation is induced by HRF in naive mice in an Fc receptor–dependent manner.Naive WT C57BL/6 and mutant mice were treated i.n. with 40 μg mHRF-His_6 3 times every third day. PBS served as a negative control. (**A** and **B**) HRF-induced lung inflammation required B and mast cells as well as FcεRI (and probably Fcγ receptors). BAL procedures were conducted 24 hours after the last HRF administration. Differential cell counting was performed on cytospin preparations stained with May-Giemsa. (**C**) Genes whose expression was up- or downregulated by HRF. Black symbols, ≤3-fold change; orange symbols, 3- to 5-fold change; red symbols, >5-fold change. Genes whose expression fluctuated ≤3-fold in WT, *FcεRIα*$^{-/-}$, and *FcRγ*$^{-/-}$ mice are not shown in the plots for the mutant mice. Dashed and solid lines indicate 3- and 5-fold differences, respectively, in gene expression. $*P < 0.05$, $**P < 0.01$, $***P < 0.001$, Student's *t* test. Each cohort consisted of 3–5 mice. All data are representative of 5 (WT) and 2 (mutant) experiments.

Importantly, the absence of inflammatory cell responses to HRF in *μMT* or *FcRγ*$^{-/-}$ mice corroborated our finding that HRF bound Igs (Figure 1). To further evaluate the target range of HRF, we performed global gene expression analysis. Expression of 196 genes was up- or downregulated more than 3-fold by HRF in the lungs of naive WT mice, with 90 genes up- or downregulated more than 5-fold (Figure 7C). Upregulated genes included those encoding Th1-, Th2-, and Th17-associated cytokines and various chemokines, potentially accounting for the recruitment of monocytes/macrophages, neutrophils, eosinophils, and other immune cells (Supplemental Figure 16). Expression of some Th1 and Th2 cytokines were confirmed by real-time PCR analysis (data not shown). Other upregulated genes included the previously reported genes in mouse asthma models, such as *Agr2*, *Ccl8*, *Ccl11*, *Fcgr2b*, *Scin*, *Serpina3g*, *Serpina3n*, and *Timp1*. However, only a small fraction of these genes (39 of 196) fluctuated more than 3-fold in *FcεRIα*$^{-/-}$ mice; furthermore, fewer genes (11 of 196) were changed in *FcRγ*$^{-/-}$ mice (Figure 7C). These results suggest that HRF executes its action largely, if not exclusively, by engaging IgE- and IgG-bound Fc receptors and promotes airway inflammation.

Discussion

Despite considerable efforts in the last 15 years since the cloning of HRF (4), the receptor for HRF has not been identified. Using functional assays on RBL-2H3 rat mast cells expressing human FcεRI, Wantke et al. indirectly suggested that human recombinant HRF does not bind to IgE (34). However, we clearly demonstrated that a subset of IgE and IgG can interact with HRF. Our study differs from that of Wantke et al., as theirs used human FcεRI-expressing RBL-2H3 cells, which in our hands were difficult to activate. Importantly, we used more than a dozen IgE mAbs in an ELISA-based binding assay, compared with 2 types of polyclonal IgE used in the prior study. Furthermore, HRF binding of some IgE mAbs was confirmed by affinity pulldown and flow cytometry.

HRF interacts with the Fab, but not Fc, region of Igs. Experiments with OVA antigen and monovalent haptens suggested that the mHRF-binding site in IgE overlaps at least in part with the antigen-binding sites. Inspection of amino acid sequences of V regions of a limited number of IgE and IgG molecules indicates that HRF-reactive IgEs and IgGs contain unique V_k sequences (8–30 and 2–137, respectively; Supplemental Table 1). In contrast, these IgEs and IgGs use different V_H family members. The Ig-binding N19 peptide forms 2 antiparallel β-sheets (positions 3–5 and 14–15), which, together with the C-terminal β-sheet, form the 3-stranded sheet B (54, 55). The structure consisting of sheet B, the 4-stranded sheet A, and the small helix is similar to that of the human protein Mss4, which binds to Rab proteins and is proposed to be a guanine nucleotide-free chaperone (56). The other Ig-interacting H3 domain is a long α-helix packed against part of sheet A. Our observations collectively suggest that 2

J. in:
- JCI | PubMed | Google Scholar
- Find articles by **Kawakami, T.** in:
- JCI | PubMed | Google Scholar

Go to
- Top
- Abstract
- Introduction
- Results
- Discussion
- Methods
- Supplemental material
- References

Need help?
- E-mail the JCI

sites of HRF interact with V regions specifically. However, data on hapten inhibition of HRF-Ig interactions cannot rule out the possibility that HRF-Ig binding is enacted by relatively nonspecific ionic or other interactions of different parts of Igs.

As shown by others (57, 58), our bacterially expressed mHRF preparations can form a dimer. HRF has 2 Ig-binding sites at the N19 and H3 peptide regions. Our present biochemical analyses suggested that an HRF dimer can aggregate 2 or 4 FcεRI complexes preloaded with IgE (Supplemental Figure 8B). As a dimer is the minimal FcεRI complex required for cell activation (59), mHRF along with HRF-reactive IgE could induce mast cell activation. Consistent with these in vitro data, FcεRI-dependent PCA-like skin inflammation and lung inflammation were induced by WT mHRF, but not the monomeric 2CA mutant mHRF.

The progress in HRF research has been hindered by the lack of identification of an HRF receptor and the lack of tools to distinguish its extracellular from intracellular HRF functions. The peptides N19 and H3 corresponding to the Ig-interacting sites within mHRF turned out to be specific inhibitors that interfered with the interactions between extracellular HRF and IgE, but had no effect on HRF's intracellular functions. The biologic activities of these peptides were shown by their suppression of in vitro mast cell activation and in vivo mast cell–dependent inflammation, i.e., PCA and airway inflammation. It should be emphasized that these peptides used as GST fusion proteins did not affect HRF's intracellular functions, as they were not taken up intracellulary. A synthetic N19 peptide also did not affect the intracellular functions. Kim et al. have shown that N10 of HRF can work as a protein translocation domain (PTD) when fused with some proteins at their N termini (60). Protein internalization by this PTD was characterized by the high dose requirement (8–32 μM) and slow kinetics compared with that of TAT, an HIV-encoded peptide (61). However, we found that the PTD function of N10 peptide in conjunction with GST (both N10-GST and GST-N10) was very weak compared with TAT-GST, particularly when N10 was fused at the C-terminus of GST (compare Supplemental Figure 7 and Figure 4A). More importantly, we clearly showed that GST-N19 and GST-H3 did not enter the mast cell or other cells.

A recent study shows that an N-terminal deletion mutant of rat HRF (Del-N11) exhibits a stronger dimerizing propensity and a stronger cytokine activity than the full-length HRF (58), consistent with our results indicating that the dimer is the biologically active form of HRF. The same study also shows that Del-N11 HRF, but not full-length HRF, induces airway inflammation, when the HRF protein is used to i.p. sensitize and then to i.n. challenge mice. Although these results are interesting, HRF was used as an antigen, similar to OVA in the acute airway inflammation experiments. Thus, the results do not necessarily represent the cytokine activity of HRF. Consistent with this interpretation, Del-N11 HRF fails to induce the recruitment of monocytes and macrophages in the acute airway inflammation experiments, which is very different from our data on airway inflammation induced by mHRF in naive mice.

Inhibition or amelioration of PCA and airway inflammation by N19 or H3 blockade of HRF-Ig interactions demonstrated that HRF plays a critical role in promoting antigen-induced inflammation. Consistent with our data, transgenic mice expressing HRF in a lung Clara cell–specific manner exhibit increased numbers of macrophages in BAL fluids in naive mice and increased airway inflammation in OVA-sensitized and OVA-challenged mice (62). However, the effect of HRF overexpression in this transgenic study could not be ascribed solely to the function of the secreted HRF molecule; the effect of the transgene could be due to the intracellular effect of HRF as well. Given our present data on the crucial role of HRF in asthma models, as well as the previous data of HRF-like activity in asthma and other allergic conditions, further studies of HRF and the utility of N19 and H3 inhibition of HRF are warranted in preclinical and clinical settings.

Airway inflammation by HRF in naive mice may be mediated predominantly by FcεRI expressed on mast cells, but not basophils, as there are normal numbers of basophils in $Kit^{W\text{–}sh/W\text{–}sh}$ mice (63). However, Fcγ receptors may also contribute to this inflammation. Abrogation of HRF-induced airway inflammation and gene modulation in naive $Fc\varepsilon RI\alpha^{-/-}$ and $Fc R\gamma^{-/-}$ mice support the notion that IgE and IgG are the long-sought receptors for HRF in the lung. Based on the profile of up- or downregulated genes, we propose the following scenario: HRF crosslinks FcεRI-bound IgE (and Fcγ receptor–bound IgG) on mast cells in

naive mice and activates the cells; activated mast cells secrete various proinflammatory mediators; these mediators then initiate inflammation by directly or indirectly recruiting various inflammatory cells. In addition, a similar HRF-mediated mechanism promotes the amplification of allergen-induced inflammation by activating mast cells and basophils, in which FcεRI complexes are occupied suboptimally with allergen-specific IgE (or, rather, occupied with nonspecific IgEs) to respond to allergen. Potentially at odds with the above scenario, sera and BAL fluids from naive mice contain HRF, which does not appear to induce inflammation under homeostatic conditions. Thus, there seem to be mechanisms to suppress inflammation potentially inducible by endogenous HRF. The endogenous amount of HRF might be lower than the threshold for HRF to induce inflammation. Alternatively, there might be endogenous inhibitors that inhibit HRF's extracellular functions. These possibilities are worthy of investigation.

In summary, our study demonstrated that the bioactive HRF (i.e., dimers and oligomers) interacted with some IgE molecules and could crosslink that IgE-bound FcεRI. FcεRI aggregates activated mast cells in vitro. Inhibitors that prevent HRF-Ig interactions suppressed IgE/antigen-induced skin hypersensitivity and allergen-induced mast cell–dependent airway inflammation. Thus, we conclude that HRF promotes allergic inflammation in the skin and lung.

Methods

Mice. C57BL/6 and Balb/c mice were purchased from the Jackson Laboratory. *FcεRIα*$^{-/-}$, *FcRγ*$^{-/-}$, and *μMT* mice were also used.

Preparation of recombinant mHRF. mHRF cDNAs were amplified by RT-PCR using the primers listed in Supplemental Table 2. GST fusion proteins were purified using glutathione-agarose (Sigma-Aldrich). mHRF-His$_6$ expressed by pET-24a(+) plasmid was purified using ProBond resin (Invitrogen). All recombinants were further purified by Sephacryl S-100 and dialyzed against PBS. mHRF-His$_6$ preparations contained less than 0.05 pg/μg protein of endotoxin, as measured by Limulus amebocyte lysate test.

ELISA. 96-well ELISA plates were coated overnight with GST, GST-mHRF, or mHRF-His$_6$ (each at 10 μg/ml in 0.1 M carbonate buffer [pH 9.5]). The plates were washed and blocked with 10% FCS or 1% BSA. Next, mouse IgE and IgG molecules (10 μg/ml), plasma (1:100–1:200 dilution), and BAL fluids (1:10 dilution) were incubated in the coated wells, after which bound IgE was detected by incubation with biotinylated anti-mouse IgE followed with HRP-conjugated streptavidin. Bound IgG was detected by incubation with HRP-conjugated anti-mouse IgG. Color was developed using TMB substrate (BD Biosciences), and absorbance at 450 nm was measured. Sources of IgE and IgG are listed in Supplemental Table 3.

Affinity pulldown of IgE with GST-mHRF. IgE mAbs (3 μg) in 100 μl of 1% Triton X-100/PBS were incubated with 10 μg of GST- or GST-mHRF–agarose beads. Bead-bound IgEs were pulled down by centrifugation. IgE and GST proteins eluted with SDS sample buffer were detected by immunoblotting with anti-mouse IgE antibody and anti-GST mAb, respectively.

Binding affinity measurement by quartz crystal microbalance method. A quartz crystal microbalance–based (QCM-based) assay was performed using Affinix Q4 apparatus (Initium Co. Ltd.) as described previously (64).

Mast cells. BMMCs were generated by culturing bone marrow cells in IL-3 (65). Peritoneal mast cells purified using anti–c-Kit Positive Selection kit (StemCell Technologies) were also used.

Growth and apoptosis of cultured cells. CHO-K1, Jurkat, and Caco-2 cells were cultured in the absence or presence of GST or GST-N19 for 4 days, and live cells were counted. Apoptosis was induced by IL-3 depletion in BMMCs for 4 days and by 800 nM H_2O_2 in

CHO-K1 cells for 2 days, and live cells were counted.

Microscopic localization of GST-N19 and other GST fusion proteins. BMMCs were incubated at 37°C with 20 or 200 μg/ml of GST or GST fusion proterin for 0–24 hours. Washed cells were settled on glass slides. After fixation, cells were permeabilized with ice-cold methanol, then stained with anti-GST followed by Alexa Fluor 488–conjugated anti-mouse IgG. ProLong Gold antifade with DAPI (Invitrogen) was used to mount the slides. Fluorescence was observed with a FLUOVIEW FV10i confocal laser scanning microscope (Olympus).

Degranulation. Mast cells were sensitized overnight with IgE. The cells were stimulated with TNP_{26}-BSA or mHRF-His_6 for 45 minutes. The amount of histamine or β-hexosaminidase in supernatants was measured.

PCA. Mice were sensitized by i.d. injection of IgE into the ear with 0.5 μg of IgE mAb. 24 hours later, Evans blue dye (i.v.) and mHRF-His_6 (10 μg, i.d.) were sequentially injected. Dye extravasated 30 minutes after mHRF challenge was measured by extracting ears in formamide. Engraftment of $Kit^{W-sh/W-sh}$ mice with BMMCs was performed 6 weeks before the experiments (66). In some experiments in which mice were stimulated without Evans blue, ear thickness was measured.

Asthma models. In the first model (42), C57BL/6 mice were sensitized with i.p. injection of OVA (10 μg) at days 0, 7, 14, 21, 28, and 35. At days 40, 43, and 46, mice were i.n. challenged with OVA (20 μg). Some mice were i.n. pretreated with 40–400 μg of GST or GST-N19 before every OVA challenge. In some experiments, 20 μg of synthetic N19 peptide or vehicle (2% DMSO) was used for pretreatment. 24 hours after the last challenge, lung function was tested using FlexiVent system (SCIREQ). Mice were sacrificed, and BAL fluids as well as blood and lung tissues were collected. Cells in BAL fluids were enumerated after staining with May-Giemsa. Paraffin-embedded lung tissues were stained with H&E and periodic acid-Schiff. Cytokines in lung homogenates were quantified by ELISA.

In the second model of asthma (47), BALB/c mice were i.n. treated with *Aspergillus fumigatus* allergen (50 μl; Greer Laboratories) or PBS 3 times per week for 3 weeks. Some mice were i.n. pretreated with GST or GST-N19 (200 μg/50 μl) beginning at the second week for 30 minutes before each immunization. 24 hours after the last challenge, mice were sacrificed.

In the third model (48), C57BL/6 mice were i.p. immunized with OVA in the presence of alum on days 0 and 12. Mice were i.n. administered with OVA (20 μg/20 μl) on days 24, 26, and 28. Some mice were i.n. pretreated with GST or GST-N19 (400 μg/20 μl) before each OVA challenge. 24 hours after the last challenge, mice were sacrificed.

Oligonucleotide microarray. Total RNA was extracted from lungs using RNeasy Total RNA Mini Kit (Qiagen). A microarray analysis was performed using 200 ng of total RNA from each sample and SurePrint G3 Mouse Gene Expression 8x60K arrays (Agilent Technologies) according to the manufacturer's instructions. The microarray data have been deposited in Gene Expression Omnibus (GEO; accession no. GSE34133; http://www.ncbi.nlm.nih.gov/geo/query/acc.cgi?acc=GSE34133). Data analysis was performed with GeneSpring software (version GX 10.3). Because the expression levels of housekeeping genes (*GAPDH* and β-*actin*) did not differ among all samples, specific normalization was not performed. To eliminate genes containing only a background signal, genes were selected only if the raw values of "Expression" were more than 100. In addition, we focused on probes with reliable annotations (https://earray.chem.agilent.com/earray/) in the present study. A total of 16,374 genes met these criteria and were subjected to further analysis.

Statistics. Bonferroni correction was used for AHR analysis. Other statistical analyses were performed by 2-tailed Student's *t* test. Data shown indicate mean ± SEM. A *P* value less than 0.05 was considered significant.

Study approval. Animal experiments were approved by the Animal Care and Use Committee

of the La Jolla Institute for Allergy and Immunology.

Supplemental data

View Supplemental data

Acknowledgments

We thank Jae-Youn Cho and Peter Rosenthal for superb technical assistance and Shane Crotty and Howard M. Grey for critically reading this manuscript. This study was supported in part by grants from the NIH (to T. Kawakami) and the National Institute of Biomedical Innovation (ID10-43; to K. Matsumoto). This is Publication 1262 from the La Jolla Institute for Allergy and Immunology.

Footnotes

Conflict of interest: Tomomitsu Ozeki is employed by ULVAC Inc.

Citation for this article: *J Clin Invest.* 2012;122(1):218–228. doi:10.1172/JCI59072.

Miho Kimura's present address is: Department of Rheumatology and Infectious Diseases, Kitasato University School of Medicine, Sagamihara, Japan.

Jiro Kitaura's present address is: Division of Cellular Therapy, Institute of Medical Science, University of Tokyo, Tokyo, Japan.

References

1. Galli SJ, Kalesnikoff J, Grimbaldeston MA, Piliponsky AM, Williams CM, Tsai M. Mast cells as "tunable" effector and immunoregulatory cells: recent advances. *Annu Rev Immunol.* 2005;23:749–786.
   View this article via: PubMed CrossRef
2. Thueson DO, Speck LS, Lett-Brown MA, Grant JA. Histamine-releasing activity (HRA). I. Production by mitogen- or antigen-stimulated human mononuclear cells. *J Immunol.* 1979;123(2):626–632.
   View this article via: PubMed
3. MacDonald SM. Histamine releasing factors. In: Razin E, Rivera J, eds. *Signal Transduction in Mast Cells and Basophils* . New York, New York, USA: Springer-Verlag; 1999:390–401.
4. MacDonald SM, Rafnar T, Langdon J, Lichtenstein LM. Molecular identification of an IgE-dependent histamine-releasing factor. *Science.* 1995;269(5224):688–690.
   View this article via: PubMed
5. Bohm H, et al. The growth-related protein P23 of the Ehrlich ascites tumor: translational control, cloning and primary structure. *Biochem Int.* 1989;19(2):277–286.
   View this article via: PubMed
6. Chitpatima ST, Makrides S, Bandyopadhyay R, Brawerman G. Nucleotide sequence of a major messenger RNA for a 21 kilodalton polypeptide that is under translational control in mouse tumor cells. *Nucleic Acids Res.* 1988;16(5):2350.
   View this article via: PubMed CrossRef
7. Li F, Zhang D, Fujise K. Characterization of fortilin, a novel antiapoptotic protein. *J Biol Chem.* 2001;276(50):47542–47549.
   View this article via: PubMed CrossRef
8. Bommer UA, Thiele BJ. The translationally controlled tumour protein (TCTP). *Int J Biochem Cell Biol.* 2004;36(3):379–385.
   View this article via: PubMed CrossRef
9. MacDonald SM. Histamine-releasing factors. *Curr Opin Immunol.* 1996;8(6):778–783.
   View this article via: PubMed CrossRef

10. Warner JA, Pienkowski MM, Plaut M, Norman PS, Lichtenstein LM. Identification of histamine releasing factor(s) in the late phase of cutaneous IgE-mediated reactions. *J Immunol.* 1986;136(7):2583–2587.
View this article via: PubMed
11. MacDonald SM, et al. Studies of IgE-dependent histamine releasing factors: heterogeneity of IgE. *J Immunol.* 1987;139(2):506–512.
View this article via: PubMed
12. MacDonald SM. *Histamine Releasing Factors And Ige Heterogeneity* . St Louis, Missouri, USA: Mosby-Year Book Inc; 1993.
13. Telerman A, Amson R. The molecular programme of tumour reversion: the steps beyond malignant transformation. *Nat Rev Cancer.* 2009;9(3):206–216.
View this article via: PubMed CrossRef
14. Thiele H, Berger M, Skalweit A, Thiele BJ. Expression of the gene and processed pseudogenes encoding the human and rabbit translationally controlled tumour protein (TCTP). *Eur J Biochem.* 2000;267(17):5473–5481.
View this article via: PubMed
15. Guillaume E, et al. Cellular distribution of translationally controlled tumor protein in rat and human testes. *Proteomics.* 2001;1(7):880–889.
View this article via: PubMed CrossRef
16. Bommer UA, et al. The mRNA of the translationally controlled tumor protein P23/TCTP is a highly structured RNA, which activates the dsRNA-dependent protein kinase PKR. *RNA.* 2002;8(4):478–496.
View this article via: PubMed CrossRef
17. Tuynder M, et al. Biological models and genes of tumor reversion: cellular reprogramming through tpt1/TCTP and SIAH-1. *Proc Natl Acad Sci U S A.* 2002;99 (23):14976–14981.
View this article via: PubMed CrossRef
18. Cans C, et al. Translationally controlled tumor protein acts as a guanine nucleotide dissociation inhibitor on the translation elongation factor eEF1A. *Proc Natl Acad Sci U S A.* 2003;100(24):13892–13897.
View this article via: PubMed CrossRef
19. Fleischer TC, Weaver CM, McAfee KJ, Jennings JL, Link AJ. Systematic identification and functional screens of uncharacterized proteins associated with eukaryotic ribosomal complexes. *Genes Dev.* 2006;20(10):1294–1307.
View this article via: PubMed
20. Langdon JM, Vonakis BM, MacDonald SM. Identification of the interaction between the human recombinant histamine releasing factor/translationally controlled tumor protein and elongation factor-1 delta (also known as eElongation factor-1B beta). *Biochim Biophys Acta.* 2004;1688(3):232–236.
View this article via: PubMed
21. Hsu YC, Chern JJ, Cai Y, Liu M, Choi KW. Drosophila TCTP is essential for growth and proliferation through regulation of dRheb GTPase. *Nature.* 2007;445(7129):785–788.
View this article via: PubMed CrossRef
22. Dong X, Yang B, Li Y, Zhong C, Ding J. Molecular basis of the acceleration of the GDP-GTP exchange of human ras homolog enriched in brain by human translationally controlled tumor protein. *J Biol Chem.* 2009;284(35):23754–23764.
View this article via: PubMed CrossRef
23. Zhang D, Li F, Weidner D, Mnjoyan ZH, Fujise K. Physical and functional interaction between myeloid cell leukemia 1 protein (MCL1) and Fortilin. The potential role of MCL1 as a fortilin chaperone. *J Biol Chem.* 2002;277(40):37430–37438.
View this article via: PubMed CrossRef
24. Liu H, Peng HW, Cheng YS, Yuan HS, Yang-Yen HF. Stabilization and enhancement of the antiapoptotic activity of mcl-1 by TCTP. *Mol Cell Biol.* 2005;25(8):3117–3126.
View this article via: PubMed CrossRef
25. Yang Y, et al. An N-terminal region of translationally controlled tumor protein is required for its antiapoptotic activity. *Oncogene.* 2005;24(30):4778–4788.
View this article via: PubMed CrossRef
26. Susini L, et al. TCTP protects from apoptotic cell death by antagonizing bax function. *Cell Death Differ.* 2008;15(8):1211–1220.
View this article via: PubMed CrossRef
27. Rho SB, et al. Anti-apoptotic protein TCTP controls the stability of the tumor

suppressor p53. *FEBS Lett.* 2011;585(1):29–35.
View this article via: PubMed CrossRef

28. Gachet Y, Tournier S, Lee M, Lazaris-Karatzas A, Poulton T, Bommer UA. The growth-related, translationally controlled protein P23 has properties of a tubulin binding protein and associates transiently with microtubules during the cell cycle. *J Cell Sci.* 1999;112(pt 8):1257–1271.
View this article via: PubMed
29. Fenner BJ, Scannell M, Prehn JH. Expanding the substantial interactome of NEMO using protein microarrays. *PLoS One.* 2010;5(1):e8799.
View this article via: PubMed CrossRef
30. Rid R, et al. H2O2-dependent translocation of TCTP into the nucleus enables its interaction with VDR in human keratinocytes: TCTP as a further module in calcitriol signalling. *J Steroid Biochem Mol Biol.* 2010;118(1–2):29–40.
View this article via: PubMed CrossRef
31. Yarm FR. Plk phosphorylation regulates the microtubule-stabilizing protein TCTP. *Mol Cell Biol.* 2002;22(17):6209–6221.
View this article via: PubMed CrossRef
32. Chen SH, et al. A knockout mouse approach reveals that TCTP functions as an essential factor for cell proliferation and survival in a tissue- or cell type-specific manner. *Mol Biol Cell.* 2007;18(7):2525–2532.
View this article via: PubMed CrossRef
33. Koide Y, et al. Embryonic lethality of fortilin-null mutant mice by BMP-pathway overactivation. *Biochim Biophys Acta.* 2009;1790(5):326–338.
View this article via: PubMed CrossRef
34. Wantke F, MacGlashan DW, Langdon JM, MacDonald SM. The human recombinant histamine releasing factor: functional evidence that it does not bind to the IgE molecule. *J Allergy Clin Immunol.* 1999;103(4):642–648.
View this article via: PubMed CrossRef
35. Langdon JM, Schroeder JT, Vonakis BM, Bieneman AP, Chichester K, Macdonald SM. Histamine-releasing factor/translationally controlled tumor protein (HRF/TCTP)-induced histamine release is enhanced with SHIP-1 knockdown in cultured human mast cell and basophil models. *J Leukoc Biol.* 2008;84(4):1151–1158.
View this article via: PubMed
36. Inagaki N, Goto S, Yamasaki M, Nagai H, Koda A. Studies on vascular permeability increasing factors involved in 48-hour homologous PCA in the mouse ear. *Int Arch Allergy Appl Immunol.* 1986;80(3):285–290.
View this article via: PubMed
37. Wershil BK, Wang ZS, Gordon JR, Galli SJ. Recruitment of neutrophils during IgE-dependent cutaneous late phase reactions in the mouse is mast cell-dependent. Partial inhibition of the reaction with antiserum against tumor necrosis factor-alpha. *J Clin Invest.* 1991;87(2):446–453.
View this article via: JCI.org PubMed CrossRef
38. Nagai H, et al. TNF-alpha participates in an IgE-mediated cutaneous reaction in mast cell deficient, WBB6F1-W/Wv mice. *Inflamm Res.* 1996;45(3):136–140.
View this article via: PubMed
39. Hsu CL, Neilsen CV, Bryce PJ. IL-33 is produced by mast cells and regulates IgE-dependent inflammation. *PLoS One.* 2010;5(8):e11944.
View this article via: PubMed CrossRef
40. Metz M, Grimbaldeston MA, Nakae S, Piliponsky AM, Tsai M, Galli SJ. Mast cells in the promotion and limitation of chronic inflammation. *Immunol Rev.* 2007;217:304–328.
View this article via: PubMed CrossRef
41. Wills-Karp M. Immunologic basis of antigen-induced airway hyperresponsiveness. *Annu Rev Immunol.* 1999;17:255–281.
View this article via: PubMed CrossRef
42. Williams CM, Galli SJ. Mast cells can amplify airway reactivity and features of chronic inflammation in an asthma model in mice. *J Exp Med.* 2000;192(3):455–462.
View this article via: PubMed CrossRef
43. Wills-Karp M, et al. Interleukin-13: central mediator of allergic asthma. *Science.* 1998;282(5397):2258–2261.
View this article via: PubMed CrossRef
44. Grunig G, et al. Requirement for IL-13 independently of IL-4 in experimental asthma.

Science. 1998;282(5397):2261–2263.
View this article via: PubMed CrossRef
45. Walter DM, et al. Critical role for IL-13 in the development of allergen-induced airway hyperreactivity. *J Immunol.* 2001;167(8):4668–4675.
View this article via: PubMed
46. Foster PS, Hogan SP, Ramsay AJ, Matthaei KI, Young IG. Interleukin 5 deficiency abolishes eosinophilia, airways hyperreactivity, and lung damage in a mouse asthma model. *J Exp Med.* 1996;183(1):195–201.
View this article via: PubMed CrossRef
47. Mathias CB, et al. IgE influences the number and function of mature mast cells, but not progenitor recruitment in allergic pulmonary inflammation. *J Immunol.* 2009;182 (4):2416–2424.
View this article via: PubMed CrossRef
48. Takeda K, et al. Development of eosinophilic airway inflammation and airway hyperresponsiveness in mast cell-deficient mice. *J Exp Med.* 1997;186(3):449–454.
View this article via: PubMed CrossRef
49. Kim HY, DeKruyff RH, Umetsu DT. The many paths to asthma: phenotype shaped by innate and adaptive immunity. *Nat Immunol.* 2010;11(7):577–584.
View this article via: PubMed CrossRef
50. Locksley RM. Asthma and allergic inflammation. *Cell.* 2010;140(6):777–783.
View this article via: PubMed CrossRef
51. Ravetch JV, Bolland S. IgG Fc receptors. *Annu Rev Immunol.* 2001;19:275–290.
View this article via: PubMed CrossRef
52. Nimmerjahn F, Bruhns P, Horiuchi K, Ravetch JV. FcgammaRIV: a novel FcR with distinct IgG subclass specificity. *Immunity.* 2005;23(1):41–51.
View this article via: PubMed CrossRef
53. Turner H, Kinet JP. Signalling through the high-affinity IgE receptor Fc epsilonRI. *Nature.* 1999;402(6760 suppl):B24–B30.
View this article via: PubMed
54. Thaw P, Baxter NJ, Hounslow AM, Price C, Waltho JP, Craven CJ. Structure of TCTP reveals unexpected relationship with guanine nucleotide-free chaperones. *Nat Struct Biol.* 2001;8(8):701–704.
View this article via: PubMed CrossRef
55. Hinojosa-Moya J, Xoconostle-Cazares B, Piedra-Ibarra E, Mendez-Tenorio A, Lucas WJ, Ruiz-Medrano R. Phylogenetic and structural analysis of translationally controlled tumor proteins. *J Mol Evol.* 2008;66(5):472–483.
View this article via: PubMed CrossRef
56. Nuoffer C, Wu SK, Dascher C, Balch WE. Mss4 does not function as an exchange factor for Rab in endoplasmic reticulum to Golgi transport. *Molecular biology of the cell.* 1997;8(7):1305–1316.
View this article via: PubMed
57. Yoon T, Jung J, Kim M, Lee KM, Choi EC, Lee K. Identification of the self-interaction of rat TCTP/IgE-dependent histamine-releasing factor using yeast two-hybrid system. *Arch Biochem Biophys.* 2000;384(2):379–382.
View this article via: PubMed CrossRef
58. Kim M, et al. Dimerization of translationally controlled tumor protein is essential for its cytokine-like activity. *PLoS One.* 2009;4(7):e6464.
View this article via: PubMed CrossRef
59. Segal DM, Taurog JD, Metzger H. Dimeric immunoglobulin E serves as a unit signal for mast cell degranulation. *Proc Natl Acad Sci U S A.* 1977;74(7):2993–2997.
View this article via: PubMed
60. Kim M, et al. A protein transduction domain located at the NH2-terminus of human translationally controlled tumor protein for delivery of active molecules to cells. *Biomaterials.* 2011;32(1):222–230.
View this article via: PubMed CrossRef
61. Nagahara H, et al. Transduction of full-length TAT fusion proteins into mammalian cells: TAT-p27Kip1 induces cell migration. *Nat Med.* 1998;4(12):1449–1452.
View this article via: PubMed
62. Yeh YC, et al. The effects of overexpression of histamine releasing factor (HRF) in a transgenic mouse model. *PLoS One.* 2010;5(6):e11077.
View this article via: PubMed CrossRef
63. Grimbaldeston MA, Chen CC, Piliponsky AM, Tsai M, Tam SY, Galli SJ. Mast cell-

deficient W-sash c-kit mutant Kit W-sh/W-sh mice as a model for investigating mast cell biology in vivo. *Am J Pathol.* 2005;167(3):835–848.
View this article via: PubMed CrossRef

64. Ozeki T, et al. Surface-bound casein modulates the adsorption and activity of kinesin on SiO2 surfaces. *Biophys J.* 2009;96(8):3305–3318.
View this article via: PubMed CrossRef
65. Kawakami T, et al. Tyrosine phosphorylation is required for mast cell activation by Fc epsilon RI cross-linking. *J Immunol.* 1992;148(11):3513–3519.
View this article via: PubMed
66. Nakano T, et al. Fate of bone marrow-derived cultured mast cells after intracutaneous, intraperitoneal, and intravenous transfer into genetically mast cell-deficient W/Wv mice. Evidence that cultured mast cells can give rise to both connective tissue type and mucosal mast cells. *J Exp Med.* 1985;162(3):1025–1043.
View this article via: PubMed CrossRef

Identification and Functional Analysis of Novel Human Growth Hormone Secretagogue Receptor (*GHSR*) Gene Mutations in Japanese Subjects with Short Stature

Hiroshi Inoue, Natsumi Kangawa, Atsuko Kinouchi, Yukiko Sakamoto, Chizuko Kimura, Reiko Horikawa, Yosuke Shigematsu, Mitsuo Itakura, Tsutomu Ogata, and Kenji Fujieda,[†] on behalf of the Japan Growth Genome Consortium

Diabetes Therapeutics and Research Center (H.I.), The University of Tokushima, Tokushima 770-8503, Japan; Division of Genetic Information (H.I., N.K., A.K., Y.S., C.K., M.I.), Institute for Genome Research, The University of Tokushima, Tokushima 770-8503, Japan; Division of Endocrinology (R.H.), National Medical Center for Children and Mothers, Tokyo 157-8535, Japan; Fukui University Hospital (Y.S.), Fukui 910-8507, Japan; Department of Endocrinology and Metabolism (T.O.), National Research Institute for Child Health and Development, Tokyo 157-8535, Japan; and Department of Pediatrics (K.F.), Asahikawa Medical Collage, Asahikawa 078-8510, Japan

Context: Short stature (SS) is a multifactorial developmental condition with a significant genetic component. Recent studies have revealed that rare deleterious mutations in the GH-secretagogue receptor type 1A (*GHSR1A*) gene could be a cause of familial SS or GH deficiency.

Objective: The aim of this study was to evaluate the contribution of *GHSR1A* mutations to the molecular mechanism underlying SS in Japanese subjects.

Methods: We performed mutational screening of the *GHSR1A* gene in 127 unrelated Japanese SS patients diagnosed with either isolated GH deficiency or idiopathic SS. Identified mutations were analyzed in 188 control subjects, and their functional properties were examined in a heterologous expression system.

Results: Four novel heterozygous *GHSR1A* mutations were identified (ΔQ36, P108L, C173R, and D246A). Expression studies demonstrated that these mutations had varying functional consequences: 1) all mutations showed a loss-of-function effect on the constitutive signaling activity of GHSR1A, but the degree of loss varied widely; 2) C173R caused intracellular retention of the mutated protein, resulting in total loss of receptor function; 3) P108L resulted in a large decrease in binding affinity to ghrelin, without affecting its surface expression; 4) D246A uniquely impaired agonist- and inverse agonist-stimulated receptor signaling; and 5) ΔQ36 showed only a subtle reduction in constitutive activity. The cumulative frequency of these putative functional mutations was significantly higher in the patient group than in controls (4.72 *vs.* 0.53%; $P = 0.019$; odds ratio = 9.28; 95% confidence interval, 1.10–78.0).

Conclusions: Our results suggest that *GHSR1A* mutations contribute to the genetic etiology of SS in the Japanese population. (*J Clin Endocrinol Metab* 96: E373–E378, 2011)

ISSN Print 0021-972X ISSN Online 1945-7197
Printed in U.S.A

doi: 10.1210/jc.2010-1570 Received July 8, 2010. Accepted October 8, 2010
First Published Online November 17, 2010

[†] This paper is dedicated to Professor Kenji Fujieda, who sadly passed away on March 19, 2010, during the completion of this work.

Abbreviations: CA, Constitutive activity or activities; EGFP, enhanced green fluorescent protein; ER, endoplasmic reticulum; GHD, GH deficiency; GHSR, GH secretagogue receptor; HA, hemagglutinin; luc, luciferase; SPA, [D-Arg[1], D-Phe[5], D-Trp[7,9], Leu[11]]-Substance P; SRE, serum-responsive element; SS, short stature; WT, wild-type.

Ghrelin exerts pleiotropic effects, including stimulation of GH secretion and enhancement of appetite, through binding and activation of the G protein-coupled GH-secretagogue receptor (GHSR) (1, 2). Two GHSR isoforms have been identified (3, 4); the primary GHSR1A product contains seven-transmembrane domains, whereas GHSR1B is an inactive form with five-transmembrane domains. In view of the ghrelin/GHSR pathway contributing to pituitary GH release, *GHSR1A* is a biological candidate for influencing/modulating height. However, recent genome-wide association studies (5, 6) as well as studies using selected haplotype-tagging single nucleotide polymorphisms (7, 8) did not provide evidence for association between common *GHSR1A* variants and adult or childhood height.

On the other hand, rare but functionally significant *GHSR1A* mutations were discovered in patients with familial short stature (SS) (9–11), thus shedding new light on the physiological importance of the ghrelin/GHSR system in somatic growth. Initially, two missense mutations, A204E and F279L, were identified in an obese patient and a SS child, respectively (9). A204E was subsequently found in two unrelated pedigrees with familial SS, showing a codominant mode of inheritance with incomplete penetrance and variable phenotypic expressivity (10). Functional characterization demonstrated that both mutant receptors had diminished or significantly reduced constitutive activities (CA), although they showed preserved ability to respond to ghrelin (10, 12) [a high constitutive ligand-independent signaling activity, up to ~50% of ligand-stimulated signaling, has been proven for GHSR1A in an *in vitro* setting (13, 14)]. More recently, the first case of compound heterozygosity for W2X and R237W was identified in an SS patient with partial GH deficiency (GHD) (11). In this case, transmission of the GHD phenotype suggested a recessive mode of inheritance. Expression studies showed that the nonsense W2X mutation favored complete loss-of-function, whereas R237W caused only a partial, but potentially important, loss of CA.

In this study, to facilitate elucidation of the molecular etiology of familial/genetic SS, we screened for *GHSR* mutations in a cohort of Japanese patients (n = 127) with isolated GHD or idiopathic SS.

Patients and Methods

All methods are described in more detail in the Supplemental Data (published on The Endocrine Society's Journals Online web site at http://jcem.endojournals.org).

Subjects

This study was approved by the Ethics Committee for Human Genome/Gene Research of the University of Tokushima. A total of 127 unrelated Japanese individuals, diagnosed with either isolated GHD (n = 14) or idiopathic SS (n = 113) according to established clinical criteria (10, 15), were recruited by the Japan Growth Genome Consortium, a research network of Japanese pediatric endocrinologists. Written informed consent was obtained from all participants. DNA from unrelated healthy Japanese individuals (n = 188) was used as the control.

Mutational analysis

The two *GHSR1A* coding exons were screened for mutations by sequencing (Supplemental Table 1). Frequencies of variant alleles in control subjects were determined by PCR-restriction fragment length polymorphism (Supplemental Table 2).

Transfection studies

Human *GHSR1A* cDNA was used to create either N-terminal hemagglutinin (HA)-tagged or C-terminal enhanced green fluorescent protein (EGFP)-tagged expression constructs (Supplemental Table 1). Mutations were introduced by site-directed mutagenesis. Receptor-mediated luciferase (*luc*) reporter gene assays were performed on transiently transfected HEK293A cells using either serum-responsive element (SRE)-*luc* or cAMP-responsive element-*luc* reporter (12). Whole-cell receptor binding assays were conducted using ^{125}I-labeled ghrelin. Both cell-surface and total protein expression levels of the HA-tagged receptor were determined by a cell-based ELISA (12). Immunoblotting was performed with a horseradish peroxidase-conjugated anti-HA antibody. For deglycosylation experiments, lysates were treated with endoglycosidase H or protein N-glycosidase F (PNGase F). The subcellular distribution of EGFP-tagged receptors was monitored by fluorescence microscopy. Indirect immunofluorescence was performed with an antibody against the endoplasmic reticulum (ER) marker calnexin.

Statistics

Data are presented as mean ± SD. Statistical significance was analyzed using Student's *t* test and Fisher's exact test. $P < 0.05$ was considered statistically significant.

Results

Novel *GHSR* mutations

Eight *GHSR* sequence variants were identified (Table 1), which included: 1) four novel variants affecting amino acid residues common to both the 1A and 1B isoforms [ΔQ36 (a 3-bp in-frame deletion), P108L, C173R, and D246A; Supplemental Fig. 1, A and B]; 2) a missense substitution of the 1B-specific residue (A277P); and 3) three silent changes (G57G, L118L, and R159R). Heterozygous ΔQ36 was detected in three patients as well as one control. P108L, C173R, and D246A were rare, being found in only a single patient each, all in a heterozygous condition. A277P was detected in one patient and three controls. According to the SIFT and PolyPhen results, P108L and C173R were predicted as having a potentially damaging effect on protein function (Table 1).

TABLE 1. Summary information on *GHSR* variants detected in Japanese population

Exon	Sequence variant	Nucleotide change	dbSNP	Frequency		Possible functional impact			Conservation DNA/protein
				Patients (n = 127)	Controls (n = 188)	Protein level SIFT/Polyphen	RNA level		
							Splice	ESE/ESS	
1	ΔQ36	c.106-108 del CAG		0.012 (3 het)	0.003 (1het)	NA	No		No/no
1	G57G	c.171C>T	rs495225	0.667	NA	NA	Possible	Possible/possible	No/yes
1	P108L	c.323C>T		0.004 (1 het)	0	Deleterious/possibly damaging	No	Possible/no	Yes/yes
1	L118L	c.354C>T	rs2232167	0.059	NA	NA	No	No/no	Yes/yes
1	R159R	c.477G>A	rs572169	0.357	NA	NA	No	Possible/possible	Yes/no
1	C173R	c.517T >C		0.004 (1 het)	0	Deleterious/possibly damaging	No	Possible/no	Yes/no
1	D246A	c.737A>C		0.004 (1 het)	0	Tolerated/benign	No	Possible/no	No/no
1	A277P (1B)	c.829G>C	rs34273140	0.004 (1 het)	0.007 (3 het)	NA/benign	No	No/possible	No/NA

Variant nomenclature and amino acid number are based on NCBI RefSeq NM_198407 (*GHSR1A*) and NM_004122 (*GHSR1B*). RS number is based on the NCBI dbSNP database. Possible damaging effects of amino acid substitutions were predicted with the SIFT (http://sift.jcvi.org/) or PolyPhen (http://genetics.bwh.harvard.edu/pph/index.html) program. SIFT scores: P108L (0.01), C173R (0.01), and D246A (0.44). PolyPhen PSIC score differences: P108L (1.847), C173R (2.738), and D246A (0.860). PHAT matrix element difference: C173R (−8). The SIFT result for A277P is not shown as it was likely incorrect (low confidence). Potential splicing effects were predicted using the NNSPLICE (http://www.fruitfly.org/seq_tools/splice.html), GENSCAN (http://genes.mit.edu/GENSCAN.html), or Human Splicing Finder (http://www.umd.be/HSF/) program. Sequence conservation was investigated using the UCSC Genome Browser (http://genome.ucsc.edu/, using track Vertebrate Multiz Alignment & Conservation). ESE, Exonic splicing enhancer; ESS, exonic splicing silencer; het, heterozygote(s); NA, not assessed.

On the basis of these observations, we decided to focus our secondary efforts on the four novel *GHSR1A* mutations, ΔQ36, P108L, C173R, and D246A. The pedigrees of the six families carrying one of the selected mutations are shown in Supplemental Fig. 2. Little information was available regarding clinical and auxological variables for the propositi, their parents, and other family members. In the present cohort, the cumulative number of these alleles was six in 127 (4.72%) patients and one in 188 (0.53%) controls [$P = 0.019$ by two-tailed Fisher's exact test; odds ratio = 9.28; 95% confidence interval, 1.10–78.0; population attributable risk = 4.21%; 95% confidence interval, 0.37–8.06].

Functional characterization of *GHSR1A* mutations

Expression constructs encoding wild-type (WT) or mutant GHSR1A were used for transient expression in HEK293A cells and subsequent functional evaluation. In a SRE-*luc* reporter assay, when compared with WT or the two previously characterized mutant receptors [A204E and F279L (10, 12)], novel *GHSR1A* mutations displayed different signaling properties (Fig. 1A): 1) ΔQ36 displayed a partial but significant decrease in CA (67.5%) but showed comparable ghrelin (agonist)-induced activation and [D-Arg^1, D-Phe^5, D-Trp^{7,9}, Leu^{11}]-Substance P(SPA) (inverse agonist)-induced inhibition; 2) P108L showed a significant decrease in CA (32.0%) and a normal response against ghrelin, but had less sensitivity to SPA; 3) C173R was devoid of CA with a complete lack of response to ghrelin; and 4) D246A had reduced but significant CA (58.8%) while displaying a significantly lower response to ghrelin (even at 1 μM) and a nearly normal response to SPA. We obtained essentially the same findings in the cAMP-responsive element-*luc* reporter assay (data not shown).

In whole-cell [^{125}I]ghrelin binding assays, *GHSR1A* mutations displayed variable competition binding results (Fig. 1B): 1) ΔQ36 showed a slight increase in binding (about 1.15-fold) with similar binding affinity to WT (IC_{50} = 4.38 and 7.07 nM for ΔQ36 and WT, respectively); 2) specific binding was virtually undetectable for P108L and C173R; and 3) D246A showed reduced binding (~60%), with comparable binding affinity (IC_{50} = 3.38 nM).

Western blot analysis of WT-expressing cells showed the existence of intense, multiple immunoreactive bands (Fig. 1C). The immunoblot patterns from endoglycosidase H- and PNGase F-digested samples (Supplemental Fig. 3) suggested that: 1) the approximately 34- and 62-kDa bands most likely represent the nonglycosylated monomeric and dimeric forms, respectively; 2) the approximately 46-kDa species is the core-glycosylated monomeric form located in the ER; and 3) the broad band migrating at 60–90 kDa corresponds to the mature, terminally glycosylated, dimeric, or oligomeric forms. The ΔQ36, P108L, D246A, and F279L receptors showed a distribution and intensity of immunoreactive bands essentially similar to WT. In contrast, both C173R and A204E exhibited a selective and profound loss of intensity of 60- to 90-kDa bands, with the former being more severely affected, whereas their approximately 46-kDa species were preserved to some extent (Fig. 1C). These changes appeared to be not associated with an alteration of mRNA levels (*e.g.* decreased transcription, reduced mRNA stability), because the *GHSR1A* transgene levels of transfected cells, as assessed by quantitative RT-PCR, were not

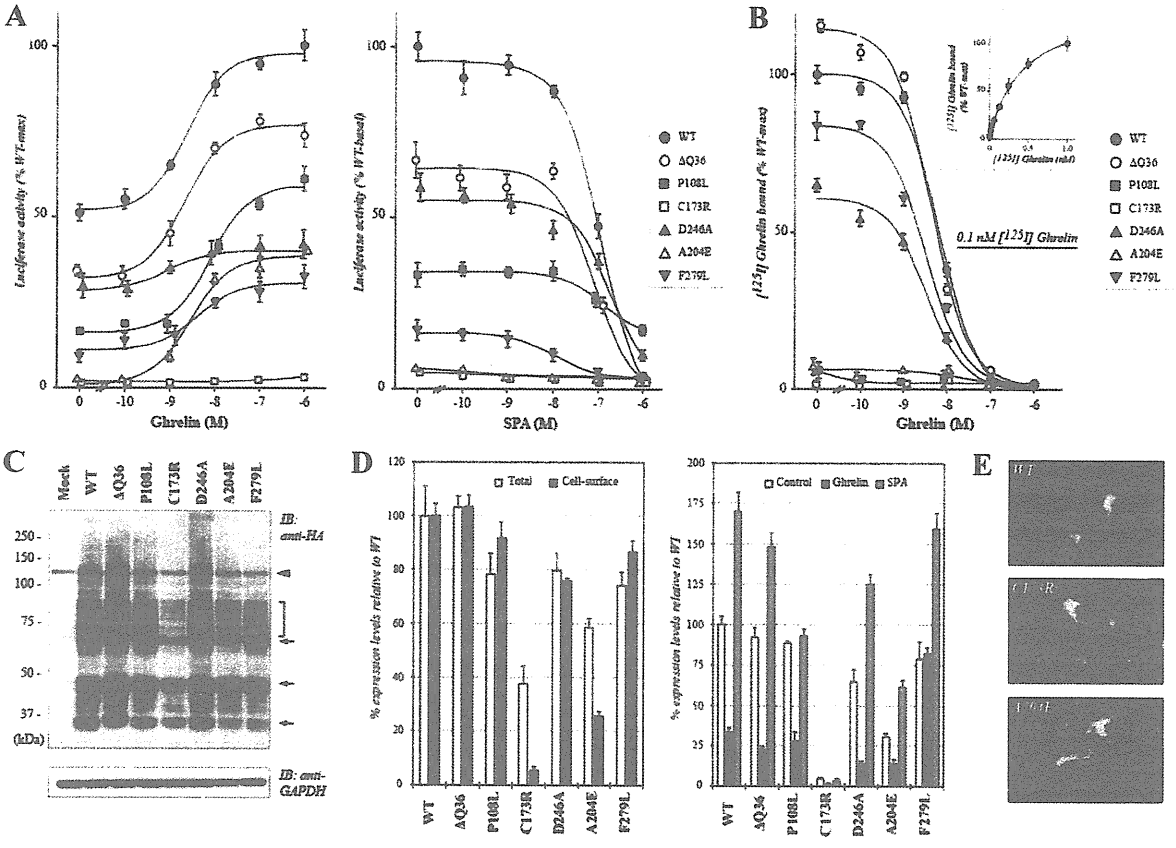

FIG. 1. Functional characterization of GHSR1A mutants. A, SRE-*luc* reporter gene assay. HEK293A cells were cotransfected with the WT or a mutant GHSR1A expression construct, pSRE-*luc* and pRL-TK plasmids, and subsequently stimulated with increasing concentrations of ghrelin (agonist; *left*) or SPA (inverse agonist; *right*). The WT receptor (*filled circles*) showed significant basal, ligand-independent CA, and treatment with ghrelin resulted in a concentration-dependent activity increase, whereas SPA inhibited CA. The two previously characterized mutant receptors, A204E (*open triangles*) and F279L (*filled inverted triangles*), showed greatly reduced CA (4.41 and 17.7%, respectively, compared with WT) but retained their ability to respond to ghrelin, these observations being consistent with previous findings (10, 12). The novel GHSR1A mutants displayed different signaling property patterns, as described in the text (ΔQ36, *open circles*; P108L, *filled squares*; C173R, *open squares*; and D246A, *filled triangles*). Transfection of vector alone resulted in no significant *luc* activity (data not shown). Results as compared with WT activity [arbitrarily set at 100, either treated with 1 μM ghrelin (*left*) or not treated (*right*)] are mean ± SD for at least four determinations. B, Whole-cell radioligand binding assay. In HEK293A cells transiently expressing the WT receptor, saturation receptor binding analysis using [^{125}I]ghrelin demonstrated a single class of high affinity, saturable binding sites with Kd of 0.43 nM, comparable to those reported in previous studies (depicted in the *inset*), whereas no specific binding was observed in cells transfected with vector alone (data not shown). Competition binding studies using 100 pM [^{125}I]ghrelin showed high affinity binding of ghrelin (IC_{50} = 7.07 nM) with the WT receptor (*filled circles*), whereas A204E (*open triangles*) displayed no detectable specific binding and F279L (*filled inverted triangles*) showed a small decrease in binding, by approximately 80%, but comparable affinity for ghrelin (IC_{50} = 3.34 nM). Newly identified GHSR1A mutants displayed variable competition binding results as described in the text (ΔQ36, *open circles*; P108L, *filled squares*; C173R, *open squares*; D246A, *filled triangles*). Results as compared with WT binding (arbitrarily set at 100), in the absence of unlabeled ghrelin, are mean ± SD for at least four determinations. C, Immunoblot (IB) analysis. N-terminally HA-tagged WT or mutated GHSR1A was transiently expressed in HEK293A cells, and whole-cell lysates were prepared. Equal protein amounts were resolved in SDS-PAGE, blotted, and probed with anti-HA antibody (*upper panel*). Glyceraldehyde-3-phosphate dehydrogenase (GAPDH) expression was evaluated as the loading control (*lower panel*). Size markers (in kilodaltons) are to the *left of the blots*. Results are representative of at least three separate independent transfection experiments yielding similar results. *Arrows* indicate major protein bands of approximately 34, 46, and 62 kDa, and *bracket* indicates a broad high molecular-weight protein band migrating between 60 and 90 kDa. *Filled triangles*, nonspecific band. D, Cell-based ELISA. *Left*, HEK293A cells were transiently transfected with N-terminally HA-tagged WT or mutated GHSR1A expression constructs. The receptor amount was measured by whole-cell ELISA assays, either in permeabilized (for total receptors; *open columns*) or nonpermeabilized (for cell-surface receptors; *black columns*) cells. Data were normalized to the WT receptor expression value and are presented as mean ± SD from three independent experiments, each performed in quadruplicate. *Right*, To evaluate the effects of agonist and inverse agonist treatment on cell-surface receptor expression, at 24 h after transfection, the medium was replaced with serum-free medium (*open columns*) and medium containing either ghrelin (1 μM; *black columns*) or SPA (1 μM; *gray columns*), and the cells were then incubated for an additional 18 h. The cell-surface receptor amounts were quantified by whole-cell ELISA assays. Data were normalized to the WT receptor expression value under the nonstimulated condition and are mean ± SD of three independent experiments, each performed in quadruplicate. Note that ghrelin treatment of WT-expressing cells resulted in significant down-regulation of cell-surface receptor expression (to ≤40% of that in corresponding nonstimulated cells), whereas, as opposed to ghrelin treatment, surface expression of the WT receptor was significantly increased when cells were exposed to SPA (by approximately 1.7-fold). E, Double immunofluorescent staining. HEK293A cells were transiently transfected with C-terminally EGFP-tagged WT (*top panel*) or mutated GHSR1A construct, either C173R (*middle panel*) or A204E (*lower panel*). The cells were fixed, permeabilized, and processed for indirect immunofluorescent staining with an antibody against calnexin, an ER marker protein. *Green* fluorescence corresponds to EGFP-GHSR1A, and *red* corresponds to calnexin. *Yellow* represents colocalization of green and red. Nuclei stained with DAPI (4′,6-diamino-2-phenylindole) are shown in *blue*.

significantly different from that of WT-expressing cells (data not shown).

The total protein expression levels of WT and mutant receptors, as assessed by a cell-based ELISA, were largely consistent with immunoblot results (Fig. 1D): 1) total cellular expression of ΔQ36 was equivalent to that of WT; 2) P108L, D246A, and F279L were expressed at a slightly reduced level (60–80%); 3) A204E exhibited significantly lower expression (<60%); and 4) C173R was expressed at the lowest level (<40%). Quantification of cell-surface receptors showed that, with respect to their total expression levels, ΔQ36, P108L, D246A, and F279L were expressed at levels approximately equal to that of WT. In contrast, C173R and A204E displayed either almost complete loss or significantly decreased surface expression (5.4 and 25.6%, respectively, compared with WT). In addition, ghrelin-induced down-regulation of ΔQ36, P108L, and D246A was comparable to that of WT, but was of a lesser degree for C173R and A204E (Fig. 1D). In contrast, the cell-surface expression of F279L did not change in response to ghrelin. The SPA-induced increase in cell surface expression of ΔQ36, D246A, A204E, and F279L, but not P108L and C173R, was comparable with that of WT.

The subcellular distributions of ΔQ36, P108L, D246A, and F279L, as monitored by fluorescence microscopy, were similar to that of WT (Supplemental Fig. 4). In contrast, both C173R and A204E displayed a fine reticular pattern of fluorescence extending from the perinuclear area and distributed throughout the cytoplasm. Double-immunofluorescent staining confirmed that the signals of C173R and A204E overlapped exclusively with that of the ER-marker, calnexin (Fig. 1E).

Discussion

We report herein the identification of four novel *GHSR1A* mutations. Functional characterization, as summarized in Supplemental Table 3, indicates that all the mutations are associated with a loss of CA, thus being consistent with a previous notion that reduced CA is responsible for SS phenotypes (10, 16). On the other hand, we found that the degree of loss could vary greatly, from only modest impairment to complete loss. Our results also highlight that *GHSR1A* mutations can have varying functional characteristics attributable to differences in their mutational mechanisms, *i.e.*: 1) P108L results in a large decrease in binding affinity to ghrelin; 2) C173R likely causes misfolding and aberrant ER retention; and 3) D246A leads to impaired agonist- and inverse agonist-stimulated receptor signaling. Notably, ΔQ36 showed only a subtle reduction in CA, thus raising the possibility that ΔQ36 may be a benign polymorphic variant. However, we cannot rule out the possibility of ΔQ36 having pathological significance, because this situation resembles the case of R237W (11), whose phenotype involves only partial loss of CA. We also provided additional information on previously identified mutations (9, 10, 12), *i.e.* A204E most likely interferes with normal intracellular trafficking resulting in ER retention, but to a much lesser extent than that of C173R, whereas F279L has impaired ability to undergo agonist-mediated receptor down-regulation, a control mechanism determining receptor responsiveness.

It should be mentioned that the *GHSR1A* mutations identified in this study occurred rarely and were each, except for ΔQ36, found only in one patient or a single family, all in a heterozygous condition, and thus their pathological significance in individual patients and families may not be sufficiently elucidated. We found the cumulative frequency of these mutations to be significantly higher in the patient group (4.72 *vs.* 0.53% in controls; $P = 0.019$), supporting that these account for a significant fraction of patients. However, obviously our sample size was small and this preliminary finding also needs to be replicated in a large and genetically homogeneous sample.

In summary, our data emphasize the importance of detailed characterization of the mutational mechanisms and functional consequences of individual *GHSR1A* mutations. Because the ghrelin/GHSR system exerts multiple biological actions in different cell types, the variability in the functional consequences of *GHSR1A* mutations may be associated with variable clinical phenotypes in patients.

Acknowledgments

We acknowledge the resources provided by the Japan Growth Genome Consortium, as well as the participating patients and their family members. We thank the many busy physicians and pediatricians who sent blood samples with clinical and biological data.

Japan Growth Genome Consortium: Department of Pediatrics, Asahikawa Medical College; Department of Endocrinology and Metabolism, National Research Institute for Child Health and Development; Saitama Children's Medical Center; Department of Pediatrics, Hokkaido University Graduate School of Medicine; Department of Pediatrics, Tendo City Hospital; Department of Pediatrics, University of Yamanashi School of Medicine; Fukui University Hospital; Department of Pediatrics, Japanese Red Cross Society Wakayama Medical Center; Department of Pediatrics, Odawara Municipal Hospital; Department of Pediatrics, Graduate School of Medicine, Kyoto University; Department of Pediatrics, Niigata Prefectural Shibata Hospital; Department of Pediatrics, Keio University School of Medicine; Department of Pediatrics, Nagasaki University School of Medicine; Department of Pediatrics, Tottori University Hospital; Department of Pediatrics, Fujieda Municipal General Hospital;